J. Chem. Sci., Vol. 120, No. 4, July 2008, pp. 363–376.

Phosphorus–nitrogen compounds: Part 15. Synthesis, anisochronism and the relationship between crystallographic and spectral data of monotopic *spiro*-crypta phosphazenes

NURAN ASMAFİLİZ[a], ELİF ECE İLTER[a], ZEYNEL KILIÇ[a,]*, TUNCER HÖKELEK[b] and ERTAN ŞAHIN[c]

[a]Department of Chemistry, Faculty of Science, Ankara University, Tandoğan, Ankara 06100, Turkey
[b]Department of Physics, Hacettepe University, Beytepe, Ankara 06800, Turkey
[c]Department of Chemistry, Faculty of Science, Atatürk University, Erzurum 25240, Turkey
e-mail: zkilic@science.ankara.edu.tr

MS received 19 March 2008; revised 16 June 2008

Abstract. The reactions of hexachlorocyclotriphosphazatriene, $N_3P_3Cl_6$, with N_2O_2-donor type coronands, $Ph_2[OR_1O][CH_2NHR_2NHCH_2]$ [$R_1 = (CH_2)_3$, $R_2 = (CH_2)_3$ (**1**), $R_1 = (CH_2)_3$, $R_2 = (CH_2)_4$ (**2**), $R_1 = (CH_2)_4$, $R_2 = (CH_2)_4$ (**3**)], give monotopic *spiro*-crypta phosphazene architectures, $N_3P_3Cl_4\{Ph_2[OR_1O][CH_2NR_2NCH_2]\}$ [$R_1 = (CH_2)_3$, $R_2 = (CH_2)_3$ (**4**), $R_1 = (CH_2)_3$, $R_2 = (CH_2)_4$ (**5**) and $R_1 = (CH_2)_4$, $R_2 = (CH_2)_4$ (**6**)], respectively. The reaction of **4** with excess pyrrolidine leads to the formation of geminal $N_3P_3Cl_2(C_5H_5N)_2\{Ph_2[O(CH_2)_3O]\ [CH_2N(CH_2)_3NCH_2]\}$ (**7**). The ^{31}P-NMR spectra of **5** and **6** indicate that these compounds have anisochronism. The structures of **5**, **6** and **7** were investigated by X-ray crystallography. For **7**, the sums of the bond angles around the N atoms were 348·6(2)° and 349·7(2)° indicating that the N atoms have pyramidal configurations and are stereogenic. The relationship between the chemical shift values $\delta P_{(spiro)}$ and the $\Delta(P–N)$ (electron density transfer parameters) of **4**, **5**, **6**, **7** and the analogous compounds as well as the relationship between the $\Delta(\delta P)$ values and the above mentioned $\Delta(P–N)$ are presented respectively. In addition, the relationship between the endocyclic NPN bond angles of these compounds and the ^{31}P-NMR chemical shifts of the *spiro*-phosphorus atoms were investigated. The spectroscopic and structural investigations of the compounds were made by elemental analyses, MS, FTIR, one-dimensional ^{1}H-, ^{13}C-, ^{31}P-NMR, DEPT and two-dimensional COSY, HETCOR, HMBC, homo- and heteronuclear correlation techniques.

Keywords. *Spiro*-crypta-phosphazenes; synthesis; anisochrony; spectroscopy.

1. Introduction

The reactions of hexachlorocyclotriphosphazatriene, $N_3P_3Cl_6$, which is known as the standard compound in the field of phosphazene and polyorganophosphazene chemistry,[1–5] with bulky bifunctional reagents lead to the formation of *spiro*-, *ansa*-, *spiro-ansa*-, *bino*-architectures and cyclolinear or cyclomatrix polymers.[6–9] The different substituents that are bonded to phosphorus atoms are very effective for the determination of the physical and chemical properties of new phosphazene derivatives and polyorganophosphazenes.[10–12] Hence, researchers have focused on the replacement reactions of halogen atoms of halophosphazenes by different nucleophiles, e.g. primary and secondary amines,[13–15] diamines,[16–18] diphenols,[19–22] diaza-crown ethers (coronands)[23–26] and aminophenols.[27] In addition, chlorophosphazene derivatives have attracted increased attention and a new class of chiral phosphazene bases have been synthesized and characterized.[28–30]

In recent years, our group has focused on the reactions of bulky bifunctional reagents, such as aromatic diamines,[31] aminophenols,[27] diphenols[32–33] and diaza-crown ethers[23–26] with $N_3P_3Cl_6$. While the reactions of aminophenols and diaza-crown ethers with $N_3P_3Cl_6$ lead respectively, to the formation of *spiro*- and *spiro*-crypta phosphazene derivatives, as major products, the condensation reaction of methylene-bis(4-nitrophenol) with $N_3P_3Cl_6$ yields the *ansa*-compound, as the major product among the *spiro*-, *spiro-spiro*- and *spiro-ansa*-skeletons.[32–33] Recently,

*For correspondence

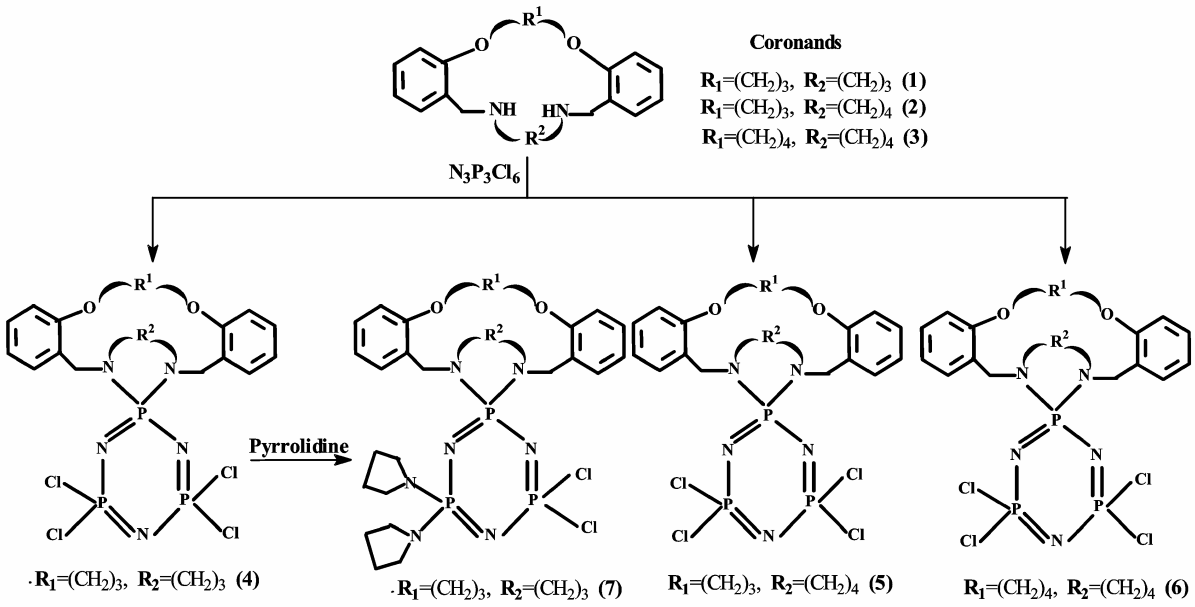

Scheme 1.

a number of interesting papers have appeared in the literature about the symmetrical[34] and unsymmetrical[35,36] *spiro*- and *ansa*-[37] phosphazene architectures.

We report here, (i) the synthesis of *spiro*-crypta phosphazenes, $N_3P_3Cl_4\{Ph_2[OR_1O][CH_2NR_2N\ CH_2]\}$ [$R_1 = (CH_2)_3$, $R_2 = (CH_2)_4$ (**5**) and $R_1 = (CH_2)_4$, $R_2 = (CH_2)_4$ (**6**)], from the reactions of $N_3P_3Cl_6$ with the coronands (bidentate diaza-crown ethers), [Ph_2 $[OR_1O][CH_2NHR_2NHCH_2]$ $R_1 = (CH_2)_3$, $R_2 = (CH_2)_4$ (**2**), $R_1 = (CH_2)_4$, $R_2 = (CH_2)_4$ (**3**)]; (ii) the substitutions of chloro atoms of $N_3P_3Cl_4\{Ph_2[O(CH_2)_3O]$ $[CH_2N(CH_2)_3NCH_2]\}$ (**4**)[24] by excess pyrrolidine that give the partly geminal substituted phosphazene $N_3P_3Cl_2(C_5H_5N)_2\{Ph_2[O(CH_2)_3O][CH_2N(CH_2)_3NCH_2]\}$ (**7**) (scheme 1); (iii) the structures of all the compounds determined by elemental analyses, mass spectrometry (MS), Fourier transform infrared spectroscopy (FTIR), one-dimensional ^{1}H-, ^{13}C and ^{31}P-NMR, distortionless enhancement by polarization transfer (DEPT), two-dimensional correlation spectroscopy (COSY), heteronuclear shift correlation (HETCOR), heteronuclear multiple-bond correlation (HMBC) homo- and heteronuclear correlation techniques; (iv) the X-ray structural analyses of **5**, **6** and **7**; (v) the relationship between the $\delta P_{(spiro)}$-shifts and the endocyclic NPN (α) bond angles, and the relationship between $\Delta(P–N)$ values and $\Delta(\delta P)$ chemical shift differences as well as $\delta P_{(spiro)}$-shifts respectively.

2. Experimental

2.1 *General techniques*

1,4-Diaminobutane and pyrrolidine were purchased from Fluka. Hexachlorocyclotriphosphazatriene was purified by crystallization from *n*-hexane. Tetrahydrofuran (THF) was dried over molecular sieves (3 Å) and the other solvents were purified according to standard procedures.[38] In the present study, because of the carcinogenic nature of benzene, toluene was chosen as the solvent in column chromatography investigations. All reactions were monitored using TLC in different solvents and purified by column chromatography using silica gel. Melting points were measured on a Gallenkamp apparatus by the use of capillary tubes. ^{1}H-, ^{13}C, ^{31}P-NMR, HETCOR, COSY, DEPT and HMBC spectra were obtained on a Bruker DPX FT-NMR (500 MHz) spectrometer ($SiMe_4$ as internal standard and 85% H_3PO_4 as an external standard). The spectrometer was equipped with a 5 mm PABBO BB inverse gradient probe. Standard Bruker pulse programs[39] were used in the experiments. FTIR spectra were obtained on a Mattson 1000 FTIR spectrometer in KBr discs. Elemental analyses were carried out by the Microanalytical Service of TUBITAK-ATAL, Ankara. Electrospray ionization mass spectra (ESI-MS) were recorded on an AGILENT 1100 MSD spectrometer.

2.2 *Synthesis of compounds*

2,6-Dioxa-14,18-diazatricyclo-[18·4·0·0^{7,12}]-tetracosa-7, 9, 11, 20, 22, 24(1)-hexaene **1**, 2,6-dioxa-14,19-diazatricyclo-[19·4·0·0^{7,12}]-pentacosa-7, 9, 11, 21, 23, 25(1)-hexaene **2** and 2,7-dioxa-15,19-diazatricyclo-[19·4·0·0^{8,13}]-pentacosa-8, 10, 12, 21, 23, 25(1)-hexaene **3**[40,41] were prepared according to the cited procedures. Also compound **4** was obtained from the reaction of **1** with $N_3P_3Cl_6$ according to the reported method.[24]

2.2a *Synthesis of 7,12-[propane-1,3-diyldioxydi-o-phenylene-dimethylene]-2,2,4,4-tetrachloro-2λ^5, 4λ^5, 6λ^5-tri phosphaza(6-P^v)-1,3,5,7,12-pentazaspiro[6·5] trideca-1,3,5-triene* (**5**): A solution of $N_3P_3Cl_6$ (3·34 g, 9·60 mmol) in dry THF (50 mL) and Et_3N (2·67 ml, 19·20 mmol) were slowly added to a solution of coronand **2** (3·00 g, 9·60 mmol) in THF (100 mL). The mixture was stirred for 2 days and the solvent was evaporated. The product was purified by column chromatography using toluene as the eluent. A white product was crystallized from ethyl acetate (yield: 2·40 g, 44%, m.p.: 215°C). Anal. Calcd. for $C_{21}H_{26}N_5O_2P_3Cl_4$: C 40·99, H 4·26, N 10·38%. Found: C 41·02, H 4·28, N 11·51%. IR (KBr, cm^{-1}, selected peaks): 3067 ν(aromatic CH asymm.), 3030 ν(aromatic CH symm.), 1242, 1182 ν(P=N), 1151 ν(C–O), 571 *s*, 509 ν(PCl_2). MS (ESI) (fragments based on ^{35}Cl, Ir%): *m/z* = 613 (M^+, 80%).

2.2b *Synthesis of 7,12-[butane-1,4-diyldioxydi-o-phenylene-dimethylene]-2,2,4,4-tetrachloro-2λ^5, 4λ^5, 6λ^5-tri phosphaza(6-P^v)-1,3,5,7,12-pentazaspiro[6·5] trideca-1,3,5-triene* (**6**): The work-up procedure is the same as that of compound **5**, using $N_3P_3Cl_6$ (2·10 g, 6·00 mmol), Et_3N (1·69 ml, 12·00 mmol) and coronand **3** (2·14 g, 6·00 mmol). The product was purified by column chromatography using toluene as the eluent and crystallized from ethyl acetate (yield: 2·00 g, 53%, m.p.: 157–159°C). Anal. Calcd. for $C_{22}H_{28}N_5O_2P_3Cl_4$: C 41·99, H 4·48, N 11·13%. Found: C 41·79, H 5·51, N 10·87%. IR (KBr, cm^{-1}, selected peaks): 3069 ν(aromatic CH asymm.), 3022 ν(aromatic CH symm.), 1236, 1176 ν(P=N), 1157 ν(C–O), 567, 511 ν(PCl_2). MS (ESI) (fragments based on 35Cl, Ir%): *m/z* = 627 (M^+, 79%).

2.2c *Synthesis of 7,11-[propane-1,3-diyldioxydi-o-phenylene-dimethylene]-2,2-dichloro-4,4-bis pyrrolidino-2λ^5,4λ^5,6λ^5-triphosphaza(6-P^v)-1, 3, 5, 7, 11-pentazaspiro[5·5] dodeca-1,3,5-triene* (**7**): A solution of compound **4** (0·45 g, 0·70 mmol) in dry THF (150 ml) was added slowly to a solution of pyrrolidine (0·70 ml, 8·40 mmol) with stirring and refluxing for 30 h. After the evaporation of THF, the mixture was dissolved in benzene (150 ml) and excess of triethylamine (0·40 ml, 3·00 mmol) was added to the solution. The mixture was refluxed for 4 h and the product was purified by coloumn chromatography using toluene/THF (5 : 1) mixture as the eluent and crystallized from *n*-heptane (yield: 0·20 g, 40%, m.p.: 163–165°C). Anal. Calcd. for $C_{28}H_{40}N_7O_2P_3Cl_2$: C 50·16, H 6·01, N 14·62%. Found: C 50·96, H 5·83, N 14·53%. IR (KBr, cm^{-1}, selected peaks): 3065 ν(aromatic CH asymm.), 3020 ν(aromatic CH symm.), 1219, 1178 ν(P=N), 1124 ν(C–O), 581, 513 ν(PCl_2). MS (ESI) (fragments based on ^{35}Cl, Ir%): *m/z* = 670 [$(MH)^+$, 100%].

2.3 *X-Ray crystallography*

Colourless crystals of **5** and **6** were crystallized from ethyl acetate, while **7** was grown from *n*-heptane at room temperature.

The molecular structures and the packing diagrams of compounds (**5**, **6** and **7**) along with the atom-numbering schemes are depicted in figures 1, 2 and 3, respectively. The crystallographic data are listed in table 1 and the selected bond lengths and angles are given in table 2. The crystallographic data were collected on a Rigaku R-AXIS RAPID-S diffractometer using MoK_α radiation (λ = 0·71073 Å) at T = 293 K. Absorption corrections by multi-scan[42] were applied. Structures were solved by direct methods[43] and refined by full-matrix least squares against F^2 using all data.[43] All non-H atoms were refined anisotropically. The H atom positions were calculated geometrically at distances of 0·93 (CH) and 0·97 Å (CH_2) from the parent C atoms; a riding model was used during the refinement process and the U_{iso}(H) values were constrained to be 1·2U_{eq} (carrier atom).

3. Results and discussion

3.1 *Synthesis*

Monotopic *spiro*-crypta phosphazenes, **5** and **6**, were synthesized from the reaction of $N_3P_3Cl_6$ with the coronands, **2** and **3** (scheme 1), in dry THF with excess Et_3N as the HCl acceptor. These reactions are likely to be regioselective, similar to the behaviour

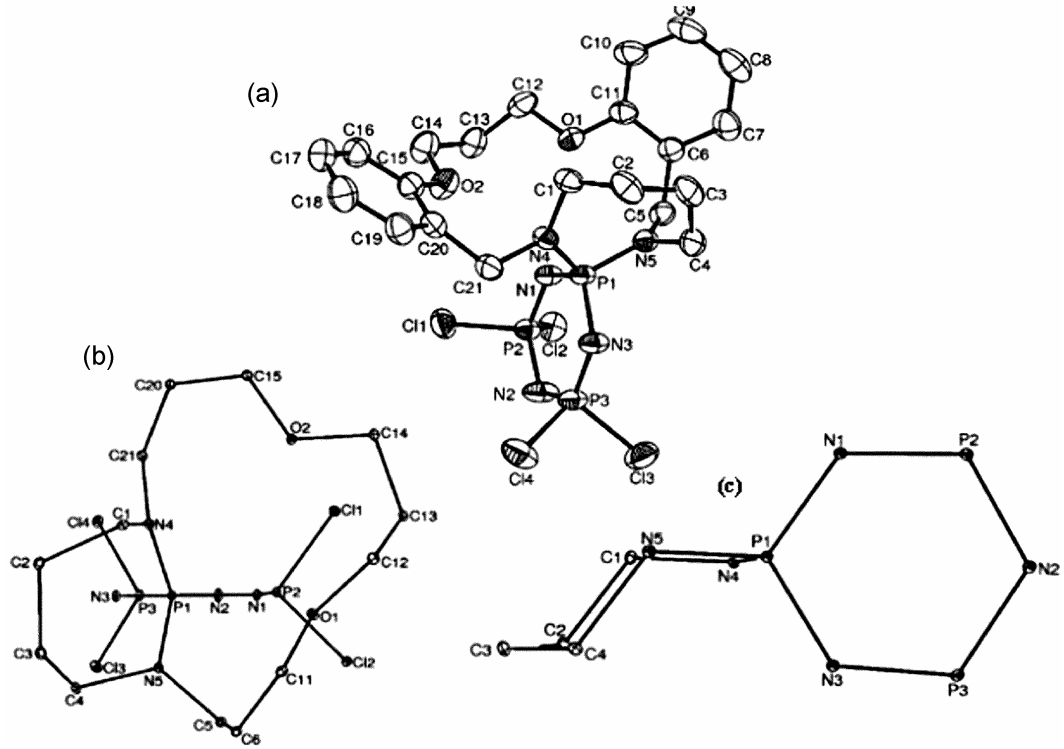

Figure 1. (**a**) An ORTEP-3[44] drawing of **5** with the atom-numbering scheme. Displacement ellipsoids are drawn at the 30% probability level. (**b**) The conformations of the phosphazene and the macro rings. (**c**) The conformation of the seven-membered *spiro*-ring.

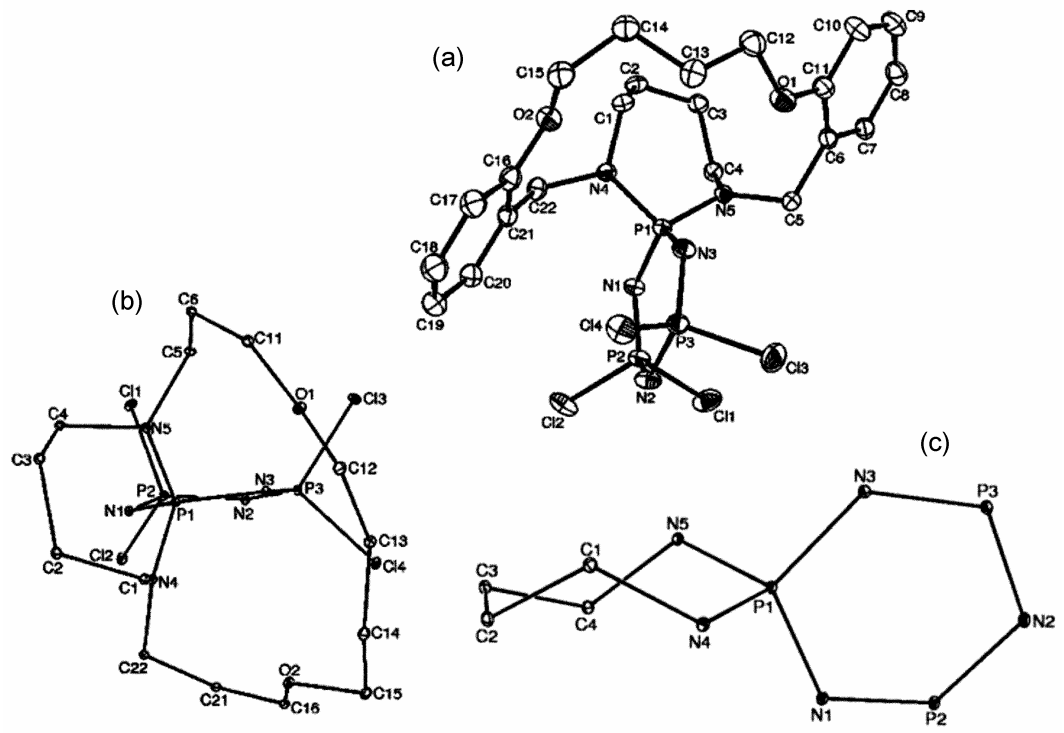

Figure 2. (**a**) An ORTEP-3[44] drawing of **6** with the atom-numbering scheme. Displacement ellipsoids are drawn at the 30% probability level. (**b**) The conformations of the phosphazene and the macro rings. (**c**) The conformation of the seven-membered *spiro*-ring.

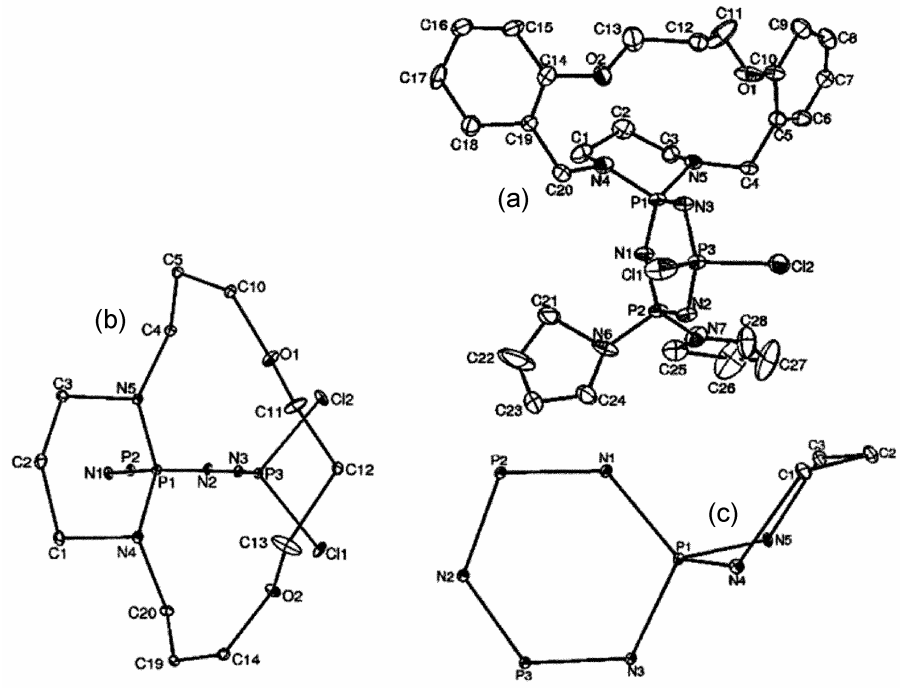

Figure 3. (**a**) An ORTEP-3[44] drawing of **7** with the atom-numbering scheme. Displacement ellipsoids are drawn at the 30% probability level. (**b**) The conformations of the phosphazene and the macro rings. (**c**) The conformation of the six-membered *spiro*-ring.

Table 1. Crystallographic data of **5**, **6** and **7**.

	(5) $C_{21}H_{26}Cl_4N_5O_2P_3$	(6) $C_{22}H_{28}Cl_{14}N_5O_2P_3$	(7) $C_{28}H_{38}Cl_{12}N_7O_2P_3$
Empirical formula	$C_{21}H_{26}Cl_{14}N_5O_2P_3$	$C_{22}H_{28}Cl_{14}N_5O_2P_3$	$C_{28}H_{38}Cl_{12}N_7O_2P_3$
Fw	615·18	629·20	668·46
Crystal system	orthorhombic	monoclinic	orthorhombic
Space group	$P2_12_12_1$	$P2_1/c$	$Pc2_1n$
a(Å)	7·9595(1)	10·019(5)	9·503(5)
b(Å)	17·8168(2)	15·369(5)	17·955(5)
c(Å)	19·3514(3)	18·682(5)	19·721(5)
α(°)	90·00	90·00	90·00
β(°)	90·00	98·679(5)	90·00
γ(°)	90·00	90·00	90·00
V(Å^3)	2744·28(6)	2843·8(19)	3365(2)
Z	4	4	4
μ(MoK) (cm^{-1})	0·636	0·615	0·703
ρ(calcd) (g cm^{-1})	1·489	1·470	1·320
Number of reflections total	75338	81976	92485
Number of reflections unique	8387	8689	9943
R_{int}	0·0517	0·0644	0·0687
$2\theta_{max}$ (°)	61·20	61·36	61·12
T_{min}/T_{max}	0·8081/0·9106	0·863/0·912	0·8081/0·9106
Number of parameters	316	326	379
R [$F^2 > 2\sigma(F^2)$]	0·0437	0·0518	0·0854
wR	0·0943	0·1372	0·2454

of homologous compounds.[23] The geminal substituted *spiro*-crypta phosphazene **7** has been prepared by means of the reaction of **4** with excess pyrrolidine. In the literature,[45–47] it is indicated that the secondary amines, e.g. pyrrolidine and diethyl amine show non-geminal bonding. However, contrarily to these observations in **7**, pyrrolidines show geminal bonding preference instead of non-geminal bonding.

Table 2. The selected bond lengths (Å) and angles (°) with the selected torsion angles (°) for **5**, **6** and **7**.

5		**6**		**7**	
P1-N1	1·610(2)	P3-N2	1·582(2)	P1-N1	1·587(3)
P1-N5	1·621(2)	P1-N4	1·624(2)	P1-N3	1·603(3)
P1-N3	1·622(2)	P3-N3	1·549(2)	P1-N4	1·609(6)
P1-N4	1·632(2)	P1-N5	1·629(2)	P1-N5	1·675(5)
P2-N1	1·5476(19)	P1-N3	1·617(2)	P3-N2	1·545(3)
P2-N2	1·577(2)	P1-N1	1·626(2)	P3-N3	1·562(3)
P2-Cl2	1·9948(10)	P2-Cl2	2·0051(11)	P3-Cl1	2·008(3)
P2-Cl1	2·0159(10)	P2-Cl1	2·0139(11)	P3-Cl2	2·023(3)
P3-N3	1·545(2)	P2-N2	1·580(2)	P2-N1	1·568(3)
P3-N2	1·586(2)	P2-N1	1·546(2)	P2-N7	1·607(8)
P3-Cl4	2·0010(11)	P3-Cl4	1·9977(11)	P2-N2	1·620(3)
P3-Cl3	2·0020(11)	P3-Cl3	2·0180(11)	P2-N6	1·645(8)
N1-P1-N3	111·88(10)	N3-P1-N1	112·32(11)	N1-P1-N3	114·35(16)
N1-P2-N2	120·41(11)	N1-P2-N2	119·93(11)	N2-P3-N3	122·77(17)
N3-P3-N2	119·80(11)	N3-P3-N2	120·10(11)	N1-P2-N2	114·01(16)
P3-N3-P1	124·89(12)	P2-N1-P1	122·57(13)	P3-N3-P1	120·18(18)
P2-N1-P1	124·58(12)	P3-N3-P1	124·31(13)	P2-N1-P1	127·7(2)
P2-N2-P3	118·25(13)	P2-N2-P3	117·10(13)	P3-N2-P2	120·51(19)
C5-N5-C4	117·4(2)	C5-N5-C4	116·50(19)	C3-N5-C4	116·4(6)
C5-N5-P1	124·61(17)	C5-N5-P1	124·08(16)	C3-N5-P1	114·1(5)
C4-N5-P1	117·80(17)	C4-N5-P1	117·31(15)	C4-N5-P1	118·1(4)
Cl-N4-C21	118·2(2)	C22-N4-Cl	117·1(2)	C20-N4-Cl	113·6(7)
Cl-N4-P1	123·97(16)	C22-N4-P1	121·00(17)	C20-N4-P1	121·2(5)
C21-N4-P1	117·27(16)	C1-N4-P1	121·66(17)	Cl-N4-P1	114·9(5)
N2-P3-N3-P1	1·4(3)	N2-P2-N1-P1	22·7(2)	N2-P2-N1-P1	4·6(8)
N1-P1-N3-P3	–0·6(2)	N3-P1-N1-P2	–11·4(2)	N3-P1-N1-P2	–6·7(9)
N2-P2-N1-P1	–4·5(3)	N2-P3-N3-P1	–0·3(2)	N3-P3-N2-P2	–6·4(8)
N3-P1-N1-P2	2·2(2)	N1-P1-N3-P3	0·3(2)	N1-P2-N2-P3	2·2(7)
N1-P2-N2-P3	4·9(3)	N1-P2-N2-P3	–21·5(2)	N2-P3-N3-P1	4·1(9)
N3-P3-N2-P2	–3·4(3)	N3-P3-N2-P2	10·6(2)	N1-P1-N3-P3	2·1(8)

The possible reasons may be; (i) the macrocycle may hinder the attack of the pyrrolidine molecule to one of the $>PCl_2$ groups, and (ii) there may be a mechanistic switch during the formation of **7**. The geminal structure of **7** has been determined by X-ray structural analyses (figure 3a).

The microanalyses, FTIR, ESI-MS spectra, NMR and crystallographic data are consistent with the proposed structures of **5**, **6**, and **7**. While the mass spectra of **5** and **6** show the molecular ion (M^+) peaks at *m*/*z* 613 and 627, the MS spectra of **7** shows a $(MH)^+$ peak at *m*/*z* 670.

3.2 *Spectroscopic analyses*

The FTIR spectra of **5**, **6** and **7** exhibit two weak intensity bands at 3069–3065 cm^{-1} and 3030–3020 cm^{-1} attributed to the asymmetric stretching vibrations of aromatic CH-bonds. Two kinds of νP=N absorption peaks are observed for mono *spiro*-crypta phosphazenes at 1242–1219 cm^{-1} and 1182–1176 cm^{-1}. The characteristic ν N–H bands of **2** (at 3412 cm^{-1}) and **3** (at 3468 cm^{-1}) disappear in the IR spectra of **5** and **6**. Two kinds of absorption frequencies for $>PCl_2$ bonds of the partially substituted phosphazenes **5**, **6** and **7** are observed in the range of 581–567 cm^{-1} and 513–509 cm^{-1}.

The proton decoupled ^{31}P-NMR spectral data of **4**,[24] **5**, **6** and **7**, and analogous *spiro*-crypta phosphazenes (**I–VII**)[23,24,26,48] are listed in table 3. The ^{31}P-NMR spectra of **5**, **6** and **7** are interpreted as ABX, ABX and AMX, respectively.

The torsion angles (table 2) indicate that the two N atoms bonded to the *spiro*-P atom are approximately perpendicular to the N_3P_3 ring (figures 1b and 2b) and in compounds **5** and **6**, its substituent R^1 and R^2 (scheme 1) project sideways, and thus the two $>PCl_2$ groups are in different environments, leading an

asymmetry. Since R^1 and R^2 differ, one might expect the anisochronism of the two $>PCl_2$ groups, as it was observed for **4**[24] and other analogous compounds (**I**, **II**, **III** and **V**).[23,24,26] The ^{31}P-NMR spectra of **5** and **6** consist of doublets of doublet for each of the phosphorus atoms, due to the anisochrony (figure 4). In addition, as expected compound **7** has also three doublets of doublet for $\delta P(pyrr)_2$ (14·30 ppm), $\delta P(spiro)$ (18·33 ppm) and δPCl_2 (27·20 ppm). In the literature,[25] for six-membered *spiro*-crypta phosphazene derivatives, it was concluded that if the $^2J_{PP}$ values are nearly the same, then the two nitrogen atoms in the *spiro*-ring have pyramidal configurations (stereogenic), if two of the $^2J_{PP}$ values are approximately the same, then one nitrogen atom has pyramidal configuration, and if all the three of the $^2J_{PP}$ values are different, then no nitrogen atom has pyramidal configuration. Compounds **5** and **6** have seven-membered *spiro*-rings and all three of the $^2J_{PP}$ values are different (table 3), hence, no nitrogen atom in the *spiro*-ring has pyramidal configuration. These findings are in accordance with the data obtained from the X-ray crystallography of **5** and **6** (the sums of the bond angles around N4 and N5 are 359·4(2)° and 359·8(2)°; 359·8(2)° and 357·9(2)°, respectively).

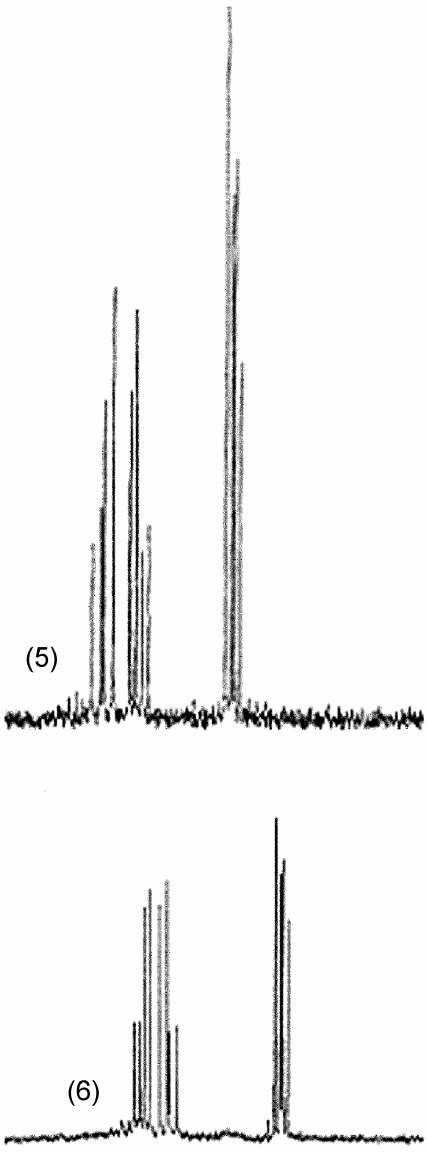

Figure 4. Anisochronism of **5** and **6**.

The α angles and the $\delta P_{(spiro)}$-shifts of the *spiro*-crypta phosphazenes (**5**, **6** and **7**) presented in this study and the analogous compounds (**4** and **I**–**VII**) taken from the literature are listed in table 3. The $\delta P_{(spiro)}$-shifts of the crypta-phosphazenes (**4**–**7** and **I**–**VII**) and the standard compound $N_3P_3Cl_6$ versus α-angles are shown in figure 5a. In this graph, one can easily observe two separate regions, A and B. In region A, monotopic tetrachloro-, and in region B, ditopic and pyrrolidinyl-substituted dichloro *spiro*-crypta phosphazenes are accumulated. These appear as a 'cluster' of points. However, a linearity between the δP-shifts and α angles has been observed for *spiro*-cyclic phosphaza lariat ethers[25] and *spiro*-cyclic (NPO) phosphazene derivatives.[49] The order of α-values are; $N_3P_3Cl_6$ > the compounds in region B cycle > the compounds in region A cycle in figure 5a.

The electron releasing or withdrawing power of the substitutents bonded to the phosphorus atoms of the N_3P_3 ring, $\Delta(P–N)$ (electron density transfer parameters: the difference between the bond lengths of two adjacent *P–N* bonds)[50,51] are also listed in table 3. The relationships between $\Delta(P–N)$ with the $\delta P_{(spiro)}$-shifts, and $\Delta(\delta P)$ values (**4**–**7** and **I**–**VII**) are illustrated in figures 5b and 5c, respectively. In figure 5b, the electron releasing power of pyrrolidinyl-substituted dichloro and ditopic *spiro*-crypta phosphazenes are greater than those of the monotopic *spiro*-crypta phosphazene derivatives. In addition, the electron releasing power of the monotopic *spiro*-crypta phosphazenes are generally in the following order; five-membered rings > six-membered rings (except III) > seven-membered rings. In this graph, the points also seem as a 'cluster'. In figure 5c, some comparisons were made on the electron releasing power of the substitutents of the phosphazenes. The macrocyclic ring and the nitrogen atoms of pyrrolidines bonded to phosphorus atoms, strongly release electrons to the phosphazene ring. For instance, the $\Delta(P–N)$ values of **4** and **7**; **III** and **IV** are respectively 0·061 and 0·058; 0·073 and 0·046, indicating

Table 3. ^{31}P-NMR (decoupled) spectral data, α angles, $\Delta(\delta P)$ and $\Delta(P–N)$ values for the compounds. [Chemical shifts (δ) are reported in ppm, J values in Hz, α angles in (°)].

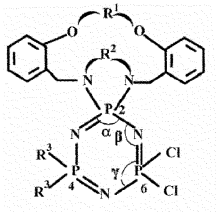

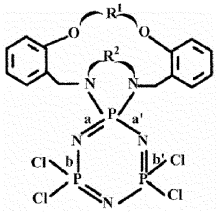

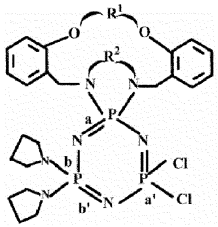

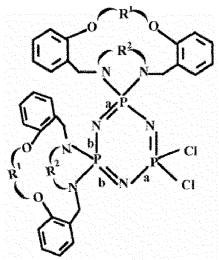

$$\Delta(P-N) = \frac{a+a'}{2} - \frac{b+b'}{2}$$

$$\Delta(P-N) = a - b$$

Compound	4[a,b,c]	5[a,c]	6[a,c]	7[a]	I[a,b,c]	II[a,b,c]	III[a,b,c]	IV[a,b]	V[a,b,c]	VI[a,b]	VII[a,b]
R^1; R^2; R^3	$(CH_2)_3$; $(CH_2)_3$; Cl	$(CH_2)_3$; $(CH_2)_4$; Cl	$(CH_2)_4$; $(CH_2)_4$; Cl	$(CH_2)_3$; $(CH_2)_3$; pyrr	$(CH_2)_3$; $(CH_2)_2$; Cl	$(CH_2CH_2)_2O$; $(CH_2)_2$; Cl	$(CH_2)_4$; $(CH_2)_3$; Cl	$(CH_2)_4$; $(CH_2)_3$; pyrr	$(CH_2CH_2)_2O$; $(CH_2)_3$; Cl	$(CH_2)_3$; $(CH_2)_3$; $(CH_2)_3$; $(CH_2)_3$; $(CH_2)_3$	$(CH_2)_4$; $(CH_2)_4$; $(CH_2)_3$; $(CH_2)_3$
$\delta(P–2)$	13·71 (*dd*) $^2J_{PP}$ = 64·1	15·31 (*dd*) $^2J_{PP}$ = 69·3	14·06 (*dd*) $^2J_{PP}$ = 71·6	18·33 (*dd*) $^2J_{PP}$ = 67·3	15·30 (*dd*) $^2J_{PP}$ = 55·4	15·50 (*dd*) $^2J_{PP}$ = 54·0	15·25 (*dd*) $^2J_{PP}$ =65·2	18·86 (*dd*) $^2J_{PP}$ = 65·7	17·15 (*dd*) $^2J_{PP}$ = 65·2	17·58 (*d*) $^2J_{PP}$ = 63·9	18·50 (*d*) $^2J_{PP}$ = 63·8
$\delta(P–4)$	17·52 (*dd*) $^2J_{PP}$ = 63·2	18·67 (*dd*) $^2J_{PP}$ = 34·4	19·07 (*dd*) $^2J_{PP}$ = 37·3	14·30 (*dd*) $^2J_{PP}$ = 24·9	21·12 (*dd*) $^2J_{PP}$ = 74·8	23·58 (*dd*) $^2J_{PP}$ = 31·4	19·35 (*dd*) $^2J_{PP}$ = 64·3	15·06 (*dd*) $^2J_{PP}$ = 36·7	19·58 (*dd*) $^2J_{PP}$ = 65·5	17·58 (*d*) $^2J_{PP}$ = 63·9	18·50 (*d*) $^2J_{PP}$ = 63·8
$\delta(P–6)$	24·71 (*dd*) $^2J_{PP}$ = 63·4	19·96 (*dd*) $^2J_{PP}$ = 52·3	20·26 (*dd*) $^2J_{PP}$ = 53·7	27·20 (*dd*) $^2J_{PP}$ = 37·5	25·52 (*dd*) $^2J_{PP}$ = 75·0	25·46 (*dd*) $^2J_{PP}$ = 78·8	25·30 (*dd*) $^2J_{PP}$ = 64·8	26·74 (*dd*) $^2J_{PP}$ = 66·3	23·50 (*dd*) $^2J_{PP}$ = 65·4	29·70 (*t*) $^2J_{PP}$ = 64·3	28·90 (*t*) $^2J_{PP}$ = 64·0
NPN(α)	111·76(11)	111·88(10)	112·32(11)	114·35(16)	111·78(10)	111·6(19)	112·5(14)	116·51(8)	111·8(2)	114·48(2)	113·97(13)
$\Delta(\delta P)$	7·41[d]	4·01[d]	5·61[d]	8·87[e]	8·02[d]	9·02[d]	7·08[d]	7·88[e]	4·24[d]	12·12[e]	10·40[e]
$\Delta(P–N)$[f]	0·061	0·069	0·074	0·058	0·055	0·053	0·073	0·046	0·069	0·026	00·40

[a] In $CDCl_3$

[b] Taken from the literature values[23,24,26,48]

[c] *P*–4 and *P*–6 values may be reversed

[d] $\Delta(\delta P)$ = average $\delta_{PCl2} - \delta_{P2}$

[e] $\Delta(\delta P) = \delta_{P6} - \delta_{P2}$

[f] $\Delta(P–N)$ = a–b (the choice of which of the two bond lengths are subtracted from each other is somewhat arbitrary, but $\Delta(P–N)$ must be consistent for the set of compounds discussed and compared)

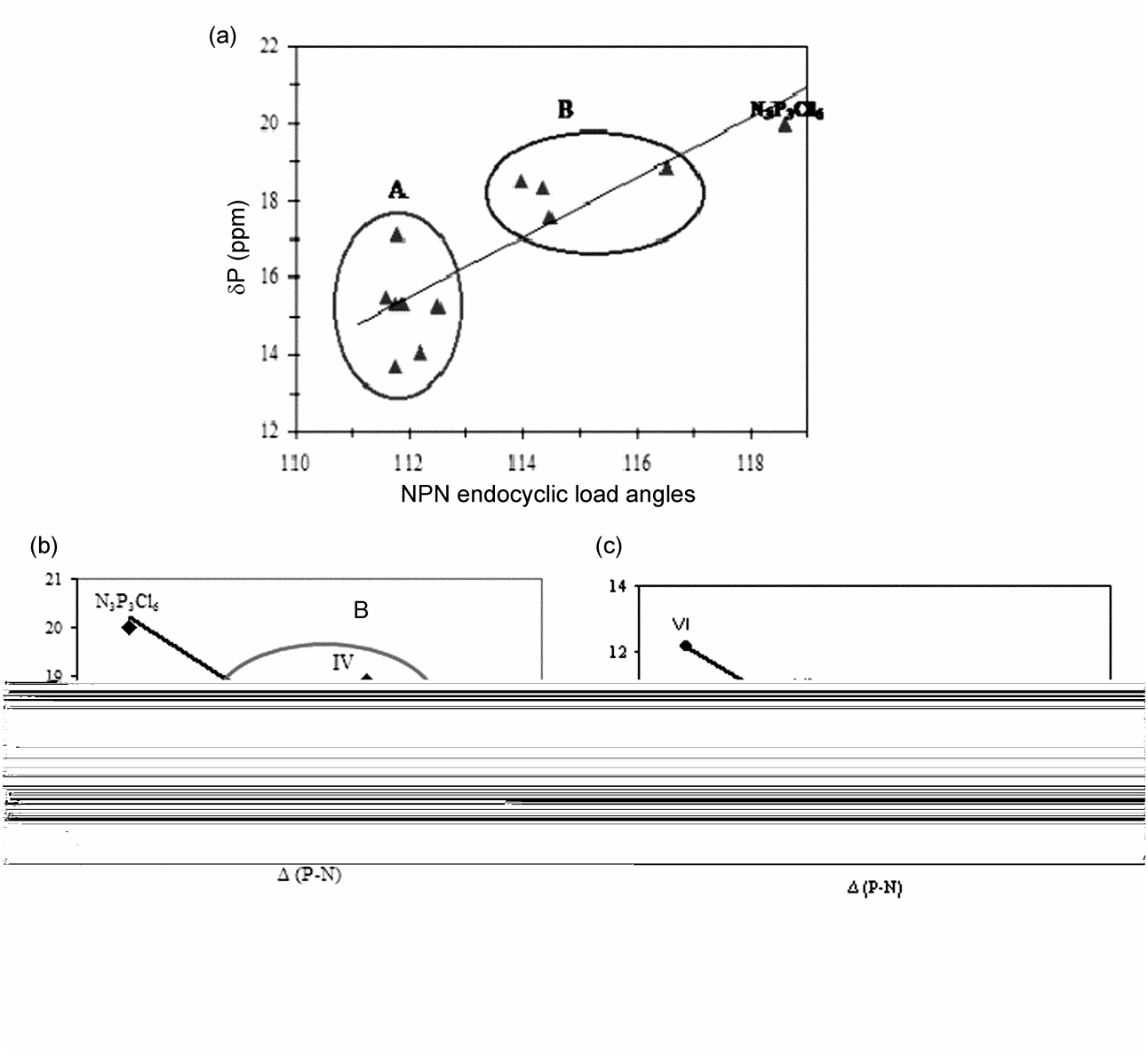

Figure 5. The relationships between (**a**) $\delta P_{(spiro)}$-values and endocyclic NPN (α) angles. (**b**) $\delta P_{(spiro)}$-values and $\Delta(P–N)$. (**c**) $\Delta(\delta P)$ values and $\Delta(P–N)$. $\delta(PCl_2)$ and the α-values of $N_3P_3Cl_6$ are 19·60 ppm, 118·30(2)°.[52] Region A indicates monotopic tetrachloro-phosphazenes, Region B indicates pyrrolidinyl-substituted and ditopic *spiro*-crypta phosphazenes.

that the electron releasing powers of pyrrolidine groups in **7** and **IV** are greater than those of the chloro groups in **4** and **III** (table 3).

In all of the *spiro*-crypta phosphazene architectures, the ^{1}H- and ^{13}C-NMR peaks were assigned on the basis of the chemical shifts, multiplicities and coupling constants (table 4). The assignments were made by HETCOR and HMBC (table 5). The HETCOR and HMBC spectra of **5** are illustrated in figures 6a and 6b, as an example, and all of the ^{1}H- and ^{13}C-NMR assignments have been written on the spectra. According to the NMR data, all the molecules appear to have symmetric structures in solution. These compounds give complex ^{1}H-NMR spectra since all of the aliphatic protons are diastereotopic. The benzylic Ar-$\underline{CH_2}$ diastereotopic protons are clearly separated from each other and can easily be distinguished. One of the peak groups is in the range of δ 3·21–3·84 ppm, while the others are in the range of δ 4·77–4·87 ppm. The benzylic protons give rise to an ABX spin system due to the geminal proton–proton coupling and the vicinal coupling

Table 4. ^{1}H- and ^{13}C-NMR (decoupled) spectral data of **5**, **6** and **7** [δ are reported in ppm, J values in Hz].

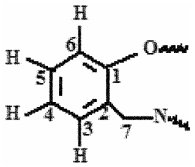

	Compounds		
	5	**6**	**7**
H3	7·15 (*dd*, 2H) ($^{3}J_{H3H4}$ = 7·1, $^{4}J_{H3H5}$ = 1·7)	7·22 (*dd*, 2H) ($^{3}J_{H3H4}$ = 7·6, $^{4}J_{H3H5}$ = 1·4)	7·13 (*dd*, 2H) ($^{3}J_{H3H4}$ = 7·4, $^{4}J_{H3H5}$ = 1·4)
H4	6·88 (*td*, 2H) ($^{3}J_{H4H3}$ = 7·1, $^{3}J_{H4H5}$ = 7·7) ($^{4}J_{H4H6}$ = 2·6)	6·93 (*td*, 2H) ($^{3}J_{H4H3}$ = 7·6, $^{3}J_{H4H5}$ = 7·1) ($^{4}J_{H4H6}$ = 1·7)	6·91 (*td*, 2H) ($^{3}J_{H4H3}$ = 7·4, $^{3}J_{H4H5}$ = 7·4) ($^{4}J_{H4H6}$ = 0·8)
H5	7·20 (*td*, 2H) ($^{3}J_{H5H4}$ = 7·7, $^{3}J_{H5H6}$ = 7·3) ($^{4}J_{H5H3}$ = 1·7)	7·29 (*td*, 2H) ($^{3}J_{H5H4}$ = 7·1, $^{3}J_{H5H6}$ = 7·4) ($^{4}J_{H5H3}$ = 1·4)	7·27 (*td*, 2H) ($^{3}J_{H5H6}$ = 7·4, $^{3}J_{H5H6}$ = 7·4) ($^{4}J_{H5H3}$ = 1·4)
H6	6·84 (*d*, 2H) $^{3}J_{H6H5}$ = 7·3	6·90 (*d*, 2H) ($^{3}J_{H6H5}$ = 7·4)	6·97 (*d*, 2H) ($^{3}J_{H6H5}$ = 7·4)
H7	3·84 (*dd*, 2H) ($^{3}J_{PH}$ = 6·8, $^{2}J_{HH}$ = 14·1) 4·77 (*dd*, 2H) ($^{3}J_{PH}$ = 11·2, $^{2}J_{HH}$ = 14·1)	3·66 (*dd*, 2H) ($^{3}J_{PH}$ = 10·2, $^{2}J_{HH}$ = 13·9) 4·80 (*dd*, 2H) ($^{3}J_{PH}$ = 9·0, $^{2}J_{HH}$ = 13·9)	3·21 (*m*, 2H) ($^{3}J_{PH}$ = 12·6) 4·87 (*dd*, 2H) ($^{3}J_{PH}$ = 12·6)
N-$\underline{CH_2}$	2·95 (*m*, 2H) 3·25 (*m*, 2H)	3·22 (*m*, 2H) 3·35 (*m*, 2H)	2·84 (*m*, 2H) 3·15 (*m*, 2H) 3·23 (*m*, 8H) (pyrr)
N-CH_2–$\underline{CH_2}$	1·17 (*m*, 2H) 1·57 (*m*, 2H)	1·06 (*m*, 2H) 1·58 (*m*, 2H)	1·37 (*m*, 2H) 1·89 (*m*, 8H) (pyrr)
O-$\underline{CH_2}$	4·18 (*m*, 2H) 4·37 (*m*, 2H)	4·13 (*m*, 4H)	4·09 (*m*, 2H) 4·29 (*m*, 2H)
O-CH_2–$\underline{CH_2}$	2·28 (*m*, 1H) 2·37 (*m*, 1H)	2·06 (*m*, 2H) 2·35 (*m*, 2H)	2·30 (*m*, 1H) 3·08 (*m*, 1H)
C1	158·0	158·2	159·1
C2	127·4 ($^{3}J_{PC}$ = 6·0)	126·5 ($^{3}J_{PC}$ = 5·5)	128·9 ($^{3}J_{PC}$ = 11·2)
C3	131·1	131·6	132·0
C4	120·7	120·3	120·9
C5	129·1	126·5	129·0
C6	113·1	112·3	117·1
C7	49·1 ($^{2}J_{PC}$ = 7·3)	50·0 ($^{2}J_{PC}$ = 7·5)	47·8 ($^{2}J_{PC}$ = 2·6)
N-$\underline{C}H_2$	46·9 ($^{2}J_{PC}$ = 6·8)	48·1 ($^{2}J_{PC}$ = 6·8)	44·7 46·3 ($^{2}J_{PC}$ = 3·7) (pyrr)
N-$CH_2\underline{C}H_2$	27·8	26·1	26·0 26·4 ($^{3}J_{P-C}$ = 9·3) (pyrr)
O-$\underline{C}H_2$	68·7	67·8	69·3
O-$CH_2\underline{C}H_2$	28·9	27·5	29·7

with the phosphorus-31 nucleus. The $^{3}J_{PH}$ for benzylic protons of **5** and **6**, which have seven-membered *spiro*-rings ($^{3}J_{PH} \approx 14{\cdot}0$ Hz), are slightly larger than those of **4**[24] and **7**, which have six-membered *spiro*-rings ($^{3}J_{PH}$ = 12·6 Hz), and **I**[24] and **II**,[26] which have five-membered *spiro*-rings ($^{3}J_{PH}$ = 10·1 Hz). In addition, the N–$\underline{CH_2}$ and N-CH_2–$\underline{CH_2}$ protons are observed at δ 2·84–3·22 ppm and δ 3·25–3·35 ppm; δ 1·06–1·37 ppm and δ 1·57–1·58 ppm, respectively as two groups of multiplets.

In ^{13}C-NMR spectra of **5** and **6** the two bond-coupling constants, $^{2}J_{PC}$ of N–$\underline{CH_2}$ (6·8 Hz for **5** and 6·8 Hz for **6**) and Ar-$\underline{CH_2}$ (7·3 Hz for **5** and 7·5 Hz for **6**) are larger than those of the three bond-coupling

Table 5. 2D ^{1}H-^{13}C HETCOR and HMBC correlations for **5**.

		HMBC [J(C, H)]				
Atom (^{1}H-NMR, ppm)	HETCOR ^{1}J	^{2}J	^{3}J	^{4}J	^{5}J	^{intra}J
H3	C3	C2, C4	C1, C5, C7	C6	C8	
H4	C4	C3, C5	C2, C6	C7	–	
H5	C5	C6, C4	C3, C1	–	–	
H6	C6	C1, C5	C4, C2	C3, C7	–	
H7 (3·84 ppm)	C7	C2	C1, C3, C8	–	C5	
H7′ (4·77 ppm)	C7	C2	C1, C3, C8	C6	C5	
H8 (2·95 ppm)	C8	C9	C7	–	–	C10
H8′ (3·25 ppm)	C8	C9	C7	–	–	
H9 (1·17 ppm)	C9	C8	–	–	–	
H9′ (1·57 ppm)	C9	C8	–	–	–	
H10 (4·18 ppm)	C10	C11	C1	–	–	
H10′ (4·37 ppm)	C10	C11	C1	C2	C3	C9
H11	C11	C10	–	–	–	C8, C9

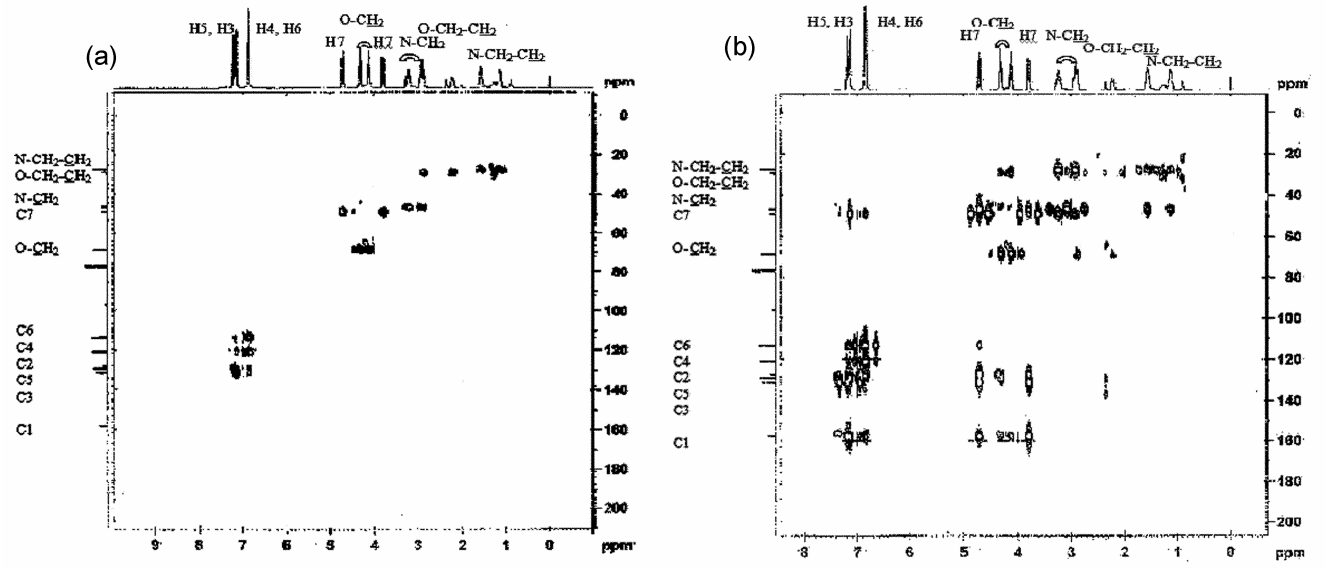

Figure 6. (**a**) The HETCOR and (**b**) HMBC spectra of compound **5**.

constants, $^{3}J_{PC}$, (6·0 Hz for **5** and 5·5 Hz for **6**) of C2 carbons. For the pyrrolidinyl-substituted phosphazene **7**, $^{2}J_{PC}$ values of N-$\underline{C}H_2$ and Ar-$\underline{C}H_2$ are much smaller than the corresponding values of **5** and **6** (table 4). In addition, the $^{2}J_{PC}$ of Ar-$\underline{C}H_2$ of the *spiro*-crypta phosphazenes are in the following order: seven-membered *spiro*-ring (**5**, **6** and $C_{22}H_{28}Cl_4N_5O_3P_3$[25]) > five-membered *spiro*-ring (**I**)[24] > six-membered *spiro*-ring (**4**, **7**, **III**, $C_{19}H_{22}Cl_4N_5O_2P_3$ and $C_{29}H_{42}Cl_2N_7O_3P_3$).[23,25] As expected, the signals of the non-protonated carbon atoms disappear in the DEPT spectrum (figure 7b), as compared with the ^{1}H-decoupled ^{13}C-NMR spectrum (figure 7a).

3.3 *X-Ray analysis of 5, 6 and 7*

In order to further corroborate the structural assignments, single crystal X-ray structures of compounds **5**, **6** and **7** are reported. The phosphazene rings of **5** and **7** are nearly planar (figures 1b and 3b), while that of **6** is not planar and is in twisted form (figure

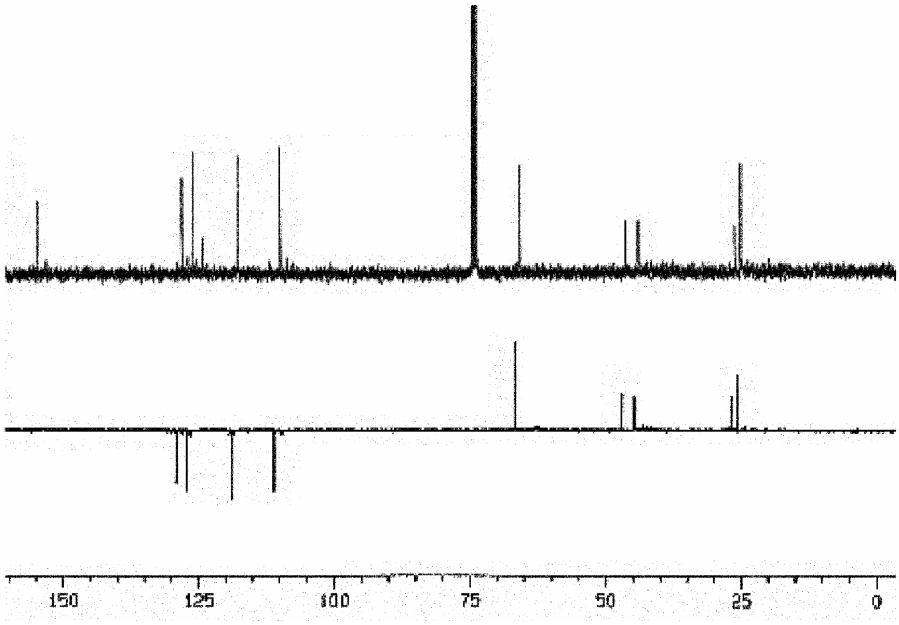

Figure 7. (**a**) The ^{13}C-NMR and (**b**) DEPT spectra of compound **5**.

2b; $\varphi_2 = -0{\cdot}2(7)°$ and $\theta_2 = 53{\cdot}3(5)°$) having total puckering amplitudes Q_T of 0·038(2), 0·181(2) and 0·075(6), for **5**, **6** and **7**, respectively.[53]

In **5**, the seven-membered ring (P1/N4/N5/C1-C4) is in chair conformation ((figure 1c); $Q_T = 0{\cdot}792(2)$ Å, $\varphi_2 = -49{\cdot}1(3)$, $\varphi_3 = -74{\cdot}4$ (2) and $\theta_2 = 36{\cdot}6(2)$]. In **6**, the seven-membered ring (P1/N4/N5/C1-C4) is in twisted form (figure 2c; $Q_T = 0{\cdot}836(2)$ Å, $\varphi_2 = 106{\cdot}0$ (2)°, $\varphi_3 = 97{\cdot}0$ (2)° and $\varphi_2 = 39{\cdot}6(2)°$). In **7**, the six-membered ring (P1/N4/N5/C1-C3) is in chair conformation (figure 3c; $Q_T = 0{\cdot}580(6)$ Å, $\varphi_2 = 169{\cdot}1(3{\cdot}9)°$ and $\theta_2 = 169{\cdot}7(7)°$). As expected, none of the macrocyclic rings are planar with the puckering amplitudes Q_T of 2·950(3) Å (for **5**), 3·804(3) Å (for **6**) and 2·510(8) Å (for **7**).

The average P–N bond lengths in phosphazene rings of **5**, **6** and **7** are 1·581(2), 1·563(2), and 1·584(3) Å, which are shorter than the average exocyclic P–N bonds of 1·627(2), 1·627(2) and 1·642(5) Å for **5**, **6** and **7**, respectively. The sum of the bond angles around the N atoms in the six and seven-membered *spiro*-cyclic rings are [359·4(2)° and 359·8(2)°] for **5**, [359·8(2) and 357·9(2)] for **6**, [348·6(2)° and 349·7(2)°] for **7**, which approve that the N atoms in **7** have pyramidal geometries. Hence, they may have stereogenic configurations, as in compound **4**.[24] As can be seen from tables 2 and 3; in **5** and **6**, α angles are narrowed, while α' and β angles are expanded considerably with respect to the corresponding values in the 'standard' compound $N_3P_3Cl_6$. In $N_3P_3Cl_6$, the α, α' and β angles are 118·3(2), 101·2(1) and 121·4(3)°, respectively.[52] In compound **7**, the α (N1–P1–N3) [114·35(16)] and γ (N1–P2–N2) [114·0(2)°] angles are narrowed, while β (P2–N1–P1) [127·7(2)°] angle is highly expanded, due to the electron back-donation of the nitrogen atoms of *spiro*- and pyrrolidine rings, as explained in figures 5b and 5c. The narrowing in the α and γ angles imply that strong electron donations from the exocyclic N atoms to the N_3P_3 phosphazene rings have occurred. The electron back-donation also causes the shortening of the exocyclic P–N bonds.

The inner hole-sizes of the macrocycles in the radii of **5**, **6** and **7**, estimated as twice the mean distance of the donor atoms from their centroids, are approximately 1·36 Å (for **5**), 1·55 Å (for **6**) and 1·46 Å (for **7**). The estimations were made by using the 'modified covalent radii' of the, N^2_{sp} (0·66 Å), N^3_{sp} (0·72 Å) and O^3_{sp} (0·76 Å), atoms as in the literature method.[54]

4. Conclusions

N_2O_2-donor type diaza crown-ethers (**1–3**) lead to the formation of monotopic *spiro*-cyclic-cryptaphosphazene architectures (**4–6**) via the condensation reactions of $N_3P_3Cl_6$. The partial substitution reaction of **4** with excess pyrrolidine results in geminal pyrrolidinyl-substituted phosphazene (**7**).

According to the ^{31}P-NMR spectra of **5** and **6**, these compounds have anisochrony. In addition, *spiro*-cyclic nitrogen atoms of **7** are stereogenic, as indicated by the X-ray crystallographic data. The variations of δP-shifts depend on the steric and electronic factors of bulky substituent, which change the α, β and γ angles of the phosphazene rings. The correlation between the endocyclic (α) angles with $\delta P_{(spiro)}$-shifts of the phosphorus atoms has been investigated. Meanwhile, the relationships between $\Delta(P–N)$ versus the $\delta P_{(spiro)}$-shifts and $\Delta(dP)$ values have been presented. No linear relationship has been observed. The points appear as a 'cluster' as given in figure 5.

Supplementary data

Crystallographic data for the structures reported here have been deposited at the CCDC as supplementary data, CCDC Nos. 666822-666824. Copies of the data can be obtained on application to CCDC, 12 Union Road, Cambridge CB2 1EZ, UK. E-mail: deposit@ccdc.cam.ac.uk.

Acknowledgements

The authors are indebted to the Department of Chemistry, Atatürk University, Erzurum, Turkey, for the use of X-ray diffractometer purchased under Grant No. 2003/219 of the University Research Fund. The authors acknowledge The Scientific and Technical Research Council of Turkey Grant No. 104T392, and Hacettepe University, Scientific Research Unit Grant No. 02 02 602 002 for financial support.

References

1. Mark J E and Allcock R W 1992 *Inorg. Polym.* Printince-Hall Englewood Cliffs NJ
2. Steiner A, Zacchini S and Richards P I 2002 *Coord. Chem. Rev.* **227** 193
3. Magro G, Donnadieu B, Spataro G, Caminade A M and Majoral J P 2007 *Polyhedron* **14** 3885
4. Heyde M, Moens M, Van Vaeck L, Shakesheff K M, Davies M C and Schacht E H 2007 *Biomacromolecules* **5** 1436
5. Allcock H R 2006 *J. Inorg. Organomet. Polym. Mater.* **4** 277
6. Wisian-Neilson P, Jung J H, Potluri S K, Mauldin C E and Zhang H 2004 *Phosphorus Sulfur Silicon Relat. Elem.* **4–5** 817
7. Benson M A, Boomishankar R, Wright D S and Steiner A 2007 *J. Organomet. Chem.* **692** 2768
8. Muralidharan K and Elias A J 2003 *Inorg. Chem.* **42** 7535
9. Raab M, Schick G, Fondermann R, Dolg M, Henze W, Weynand U, Gschwind R M and Niecke E 2006 *Angew. Chem. Int. Ed.* **19** 3083
10. Ungar G 2003 *Mol. Crys. and Liq. Cryst.* **396** 155
11. Allcock H R and Kellam III E C 2003 *Solid State Ionic* **156** 401
12. Peterson E S, Luther T A, Harrup M K, Klaehn J R, Stone M L, Orme C J and Stewart F F 2007 *J. Inorg. and Organomet. Polym. Mater.* **17** 361
13. Allen C W 1991 *Chem. Rev.* **91** 119
14. Contractor S R, Kılıç Z and Shaw R A 1987 *J. Chem. Soc., Dalton Trans.* 2023
15. Shaw R A 1980 *Pure Appl. Chem.* **52** 1063
16. Kılıç A, Kılıç Z and Shaw R A 1991 *Phosphorus Sulfur Silicon Relat. Elem.* **57** 111
17. Wilson M, Lafaille L, Vidaud L and Labarre J E 1987 *Phosphorus Sulfur Silicon Relat. Elem.* **29** 147
18. Coles S J, Davies D B, Eaton R J, Hursthouse M B, Kýlýç A, Mayer T A, Shaw R A and Yenilmez G 2002 *J. Chem. Soc., Dalton Trans.* 365
19. Yıldız M, Kılıç Z and Hökelek T 1999 *J. Mol. Struct.* **510** 227
20. Kılıç A, Begeç S, Çetinkaya B, Kılıç Z, Hökelek T, Gündüz N and Yıldız M 1996; Kılıç A, Begeç S, Çetinkaya B, Kılıç Z, Hökelek T, Gündüz N and Yıldız M 1996 *Heteroatom Chem.* **4** 249
21. Allcock H R, Sunderland N, Primrose A P, Rheingold A L, Guzei I A and Parvez M 1999 *Chem. Mater.* **11** 2478
22. Carriedo G A, Garcia Alonso F J, Gonzalez P A, Valenzuela C D and Saez N Y 2002 *Polyhedron* **21** 2579
23. İlter E E, Çaylak N, Iþıklan M, Asmafiliz, Kılıç Z and Hökelek T 2004 *J. Mol. Struct.* **697** 119
24. Asmafiliz N, İlter E E, Iþıklan M, Kılıç Z, Tercan B, Çaylak N, Hökelek T and Büyükgüngör O 2007 *J. Mol. Struct.* **832** 172
25. Bilge S, Demiriz Ş, Okumus A, Kılıç Z, Tercan B, Hökelek T and Büyükgüngör O 2006 *Inorg. Chem.* **45** 8755
26. Bilge S, Kılıç Z, Çaylak N and Hökelek T 2004 *J. Mol. Struct.* 2004 **707** 139
27. Bilge S, Natsagdorj A, Demiriz Ş, Çaylak N, Kılıç Z and Hökelek T 2004 *Helvetica Chim. Acta.* **87** 2088
28. Carriedo G A, Garcia-Alonso J F, Garcı´a-Alvarez L J, Pappalardo G C, Punzo F and Rossi P 2003 *Eur. J. Inorg. Chem.* 2413
29. Shimono S, Takahashi H, Sakai N, Tamura R, Ikuma N, Yamauchi J 2005 *Mol. Cryst. Liq. Cryst.* **440** 37
30. Gleria M and De Jaeger R 2001 *J. Inorg. Organometallic Polymers* **11** 1
31. Bilge S, Özgüç B, Demiriz Ş, İşler H, Havyalı M, Kılıç Z and Hökelek T 2005 *J. Mol. Struct.* **748** 101
32. Hökelek T, Akduran N, Yıldız M, Dal H and Kılıç Z 2000 *Acta Crystallogr.* **C56** 90
33. Öztürk L, Hökelek T, Dal H and Kılıç Z 2001 *Acta Crystallogr.* **E58** 20
34. Beşli S, Coles S J, Davarcı, D, Davies D B, Hursthouse M B and Kılıç A 2007 *Polyhedron* **26** 5283

35. Satish Kumar N and Kumara Swamy K C 2004 *Polyhedron* **23** 979
36. Bhuvan Kumar N N and Kumara Swamy K C 2008 *Chirality* **20** 781
37. Beşli S, Coles S J, Davies D B, Hursthouse M B, Kılıç A and Shaw R A 2007 *Dalton Trans.* 2792
38. Perin D D, Armarego W L and Perrin D R 1980 *Purification of laboratory chemicals* (Oxford: Pergamon), 2nd edn
39. Bruker program 1D WIN-NMR (release 6.0) and 2D WIN-NMR (release 6.1)
40. Grimsley P G, Lindoy L F, Lip 1-1 C, Smith R J and Baker J T 1977 *Aust. J. Chem.* **30** 2095
41. Adam K R, Clarkson C, Leong A J, Lindoy L F, McPartlin M, Powell H R and Smith S V 1994 *J. Chem. Soc., Dalton Trans.* 2791
42. Blessing R H 1995 *Acta Crystallogr.* **A51** 33
43. Sheldrick G M 1997 *SHELXS-97 and SHELXL-97* University of Göttingen Germany
44. Farrugia L J 1997 *J. Appl. Crystallogr.* **30** 565
45. Lensink C, de Ruiter B and van de Grampel J C 1984 *J. Chem. Soc., Dalton Trans.* 1521
46. Shaw R A 1976 *Z. Naturforsch. Teil* **B31** 641
47. Alkubaisi A H, Hursthouse M B, Shaw L S and Shaw R A 1988 *Acta Crystallogr.* **B44** 16
48. Tercan B, Hökelek T, Büyükgüngör O, Asmafiliz N, İlter E E and Kılıç Z 2005 *Acta Crystallogr.* **E61** o2145
49. İlter E E, Asmafiliz N, Kılıç Z, Iþıklan M, Hökelek T, Çaylak N and Şahin E 2007 *Inorg. Chem.* **46** 9931
50. Contractor S R, Hursthouse M B, Shaw L S and Shaw R A 1985 *Acta Crystallogr.* **B41** 122
51. Beşli S, Coles S J, Davies D B, Hursthouse M, Kılıç A, Mayer T and Shaw R A 2002 *Acta Crystallogr.* **B58** 1067
52. Bullen G J 1971 *J. Chem. Soc. A* 1450
53. Cremer D and Pople J A 1975 *J. Am. Chem. Soc.* **97** 1354
54. March J 1992 *Advanced organic chemistry reactions mechanisms and structure* (New York: Wiley) 4th edn) p. 4